KEK preprint 2002-109
Belle preprint 2002-34
UCTP-106-02

Study of $\bar{B}^0 \to D^{(*)0}\pi^+\pi^-$ Decays

Abstract

We report on a study of $\bar{B}^0 \to D^{(*)0}\pi^+\pi^-$ decays using 29.1 fb^{-1} of e^+e^- annihilation data recorded at the $\Upsilon(4S)$ resonance with the Belle detector at the KEKB storage ring. Making no assumptions about the intermediate mechanism, the branching fractions for $\bar{B}^0 \to D^0\pi^+\pi^-$ and $\bar{B}^0 \to D^{*0}\pi^+\pi^-$ are determined to be $(8.0 \pm 0.6 \pm 1.5) \times 10^{-4}$ and $(6.2 \pm 1.2 \pm 1.8) \times 10^{-4}$ respectively. An analysis of $\bar{B}^0 \to D^0\pi^+\pi^-$ candidates yields to the first observation of the color-suppressed hadronic decay $\bar{B}^0 \to D^0\rho^0$ with the branching fraction $(2.9 \pm 1.0 \pm 0.4) \times 10^{-4}$. We measure the ratio of branching fractions $\mathcal{B}(\bar{B}^0 \to D^0\rho^0)/\mathcal{B}(\bar{B}^0 \to D^0\omega) = 1.6 \pm 0.8$.

Keywords: Color-suppressed B decays, factorization, branching fraction
PACS: 13.25.Hw, 14.40.Nd

The Belle Collaboration

A. Satpathy [h,e], K. Abe [h], R. Abe [aa], T. Abe [am], I. Adachi [h], H. Aihara [an], M. Akatsu [u], Y. Asano [ar], T. Aso [aq], T. Aushev [ℓ], A. M. Bakich [aj], Y. Ban [ae], A. Bay [q], I. Bedny [b], P. K. Behera [as], A. Bondar [b], A. Bozek [y], M. Bračko [s,m], T. E. Browder [g], B. C. K. Casey [g], P. Chang [x], Y. Chao [x], K.-F. Chen [x], B. G. Cheon [ai], R. Chistov [ℓ], S.-K. Choi [f], Y. Choi [ai], Y. Choi [ai], M. Danilov [ℓ], L. Y. Dong [j], S. Eidelman [b], V. Eiges [ℓ], C. Fukunaga [ao], N. Gabyshev [h], A. Garmash [b,h], T. Gershon [h], B. Golob [r,m], J. Haba [h], T. Hara [ac], N. C. Hastings [t], H. Hayashii [v], M. Hazumi [h], I. Higuchi [am], L. Hinz [q], T. Hokuue [u], W.-S. Hou [x], H.-C. Huang [x],

T. Igaki [u], Y. Igarashi [h], T. Iijima [u], K. Inami [u], A. Ishikawa [u], R. Itoh [h], H. Iwasaki [h], Y. Iwasaki [h], H. K. Jang [ah], J. H. Kang [av], P. Kapusta [y], S. U. Kataoka [v], N. Katayama [h], H. Kawai [c], Y. Kawakami [u], N. Kawamura [a], T. Kawasaki [aa], H. Kichimi [h], D. W. Kim [ai], H. J. Kim [av], Hyunwoo Kim [o], S. K. Kim [ah], K. Kinoshita [e], S. Kobayashi [af], P. Krokovny [b], R. Kulasiri [e], S. Kumar [ad], A. Kuzmin [b], Y.-J. Kwon [av], S. H. Lee [ah], J. Li [ag], D. Liventsev [ℓ], R.-S. Lu [x], J. MacNaughton [k], G. Majumder [ak], F. Mandl [k], S. Matsumoto [d], T. Matsumoto [ao], W. Mitaroff [k], K. Miyabayashi [v], H. Miyake [ac], H. Miyata [aa], T. Mori [d], T. Nagamine [am], Y. Nagasaka [i], T. Nakadaira [an], E. Nakano [ab], M. Nakao [h], H. Nakazawa [h], J. W. Nam [ai], Z. Natkaniec [y], S. Nishida [p], O. Nitoh [ap], S. Noguchi [v], S. Ogawa [aℓ], T. Ohshima [u], T. Okabe [u], S. Okuno [n], S. L. Olsen [g], Y. Onuki [aa], W. Ostrowicz [y], H. Ozaki [h], P. Pakhlov [ℓ], H. Palka [y], C. W. Park [o], K. S. Park [ai], J.-P. Perroud [q], M. Peters [g], L. E. Piilonen [at], K. Rybicki [y], H. Sagawa [h], S. Saitoh [h], Y. Sakai [h], M. Satapathy [as], O. Schneider [q], S. Schrenk [e], C. Schwanda [h,k], S. Semenov [ℓ], K. Senyo [u], R. Seuster [g], H. Shibuya [aℓ], V. Sidorov [b], J. B. Singh [ad], N. Soni [ad], S. Stanič [ar,1], M. Starič [m], A. Sugi [u], K. Sumisawa [h], T. Sumiyoshi [ao], S. Suzuki [au], S. Y. Suzuki [h], S. K. Swain [g], T. Takahashi [ab], F. Takasaki [h], K. Tamai [h], N. Tamura [aa], J. Tanaka [an], M. Tanaka [h], G. N. Taylor [t], Y. Teramoto [ab], T. Tomura [an], K. Trabelsi [g], T. Tsuboyama [h], T. Tsukamoto [h], S. Uehara [h], K. Ueno [x], S. Uno [h], G. Varner [g], C. H. Wang [w], J. G. Wang [at], M.-Z. Wang [x], E. Won [o], B. D. Yabsley [at], Y. Yamada [h], A. Yamaguchi [am], Y. Yamashita [z], M. Yamauchi [h], H. Yanai [aa], Y. Yuan [j], C. C. Zhang [j], Z. P. Zhang [ag], and V. Zhilich [b],

[a] *Aomori University, Aomori, Japan*

[b] *Budker Institute of Nuclear Physics, Novosibirsk, Russia*

[c] *Chiba University, Chiba, Japan*

[d] *Chuo University, Tokyo, Japan*

[e] *University of Cincinnati, Cincinnati, OH, USA*

[f] *Gyeongsang National University, Chinju, South Korea*

[g] *University of Hawaii, Honolulu, HI, USA*

[h] *High Energy Accelerator Research Organization (KEK), Tsukuba, Japan*

[i] *Hiroshima Institute of Technology, Hiroshima, Japan*

[j] *Institute of High Energy Physics, Chinese Academy of Sciences, Beijing, PR China*

[k] *Institute of High Energy Physics, Vienna, Austria*

[ℓ] *Institute for Theoretical and Experimental Physics, Moscow, Russia*

[m] *J. Stefan Institute, Ljubljana, Slovenia*

[n] *Kanagawa University, Yokohama, Japan*

[o] *Korea University, Seoul, South Korea*

[p] *Kyoto University, Kyoto, Japan*

[q] *Institut de Physique des Hautes Énergies, Université de Lausanne, Lausanne, Switzerland*

[r] *University of Ljubljana, Ljubljana, Slovenia*

[s] *University of Maribor, Maribor, Slovenia*

[t] *University of Melbourne, Victoria, Australia*

[u] *Nagoya University, Nagoya, Japan*

[v] *Nara Women's University, Nara, Japan*

[w] *National Lien-Ho Institute of Technology, Miao Li, Taiwan*

[x] *National Taiwan University, Taipei, Taiwan*

[y] *H. Niewodniczanski Institute of Nuclear Physics, Krakow, Poland*

[z] *Nihon Dental College, Niigata, Japan*

[aa] *Niigata University, Niigata, Japan*

[ab] *Osaka City University, Osaka, Japan*

[ac] *Osaka University, Osaka, Japan*

[ad] *Panjab University, Chandigarh, India*

[ae] *Peking University, Beijing, PR China*

[af] *Saga University, Saga, Japan*

[ag] *University of Science and Technology of China, Hefei, PR China*

[ah] *Seoul National University, Seoul, South Korea*

[ai] *Sungkyunkwan University, Suwon, South Korea*

[aj] *University of Sydney, Sydney, NSW, Australia*

[ak] *Tata Institute of Fundamental Research, Bombay, India*

[al] *Toho University, Funabashi, Japan*

[am] *Tohoku University, Sendai, Japan*

[an] *University of Tokyo, Tokyo, Japan*

[ao] *Tokyo Metropolitan University, Tokyo, Japan*

[ap] *Tokyo University of Agriculture and Technology, Tokyo, Japan*

[aq] *Toyama National College of Maritime Technology, Toyama, Japan*

[ar] *University of Tsukuba, Tsukuba, Japan*

[as] *Utkal University, Bhubaneswer, India*

[at] *Virginia Polytechnic Institute and State University, Blacksburg, VA, USA*

[au] *Yokkaichi University, Yokkaichi, Japan*

[av] *Yonsei University, Seoul, South Korea*

1 Introduction

Exclusive hadronic decay rates provide important tests of models for B meson decay [1]. B decays to final states that include a D^0 or a D^{*0} accompanied by two charged pions are interesting, because such decays provide a precision testing ground for factorization [2], and because one can search for resonant substructure in the final state. At present, only an upper limit $\mathcal{B}(\bar{B}^0 \to D^0\pi^+\pi^-) < 1.6 \times 10^{-3}$ [3], has been measured. The $D^{(*)0}\pi^+\pi^-$ final state includes the $\bar{B}^0 \to D^{(*)0}\rho^0$ decay which has not yet been observed [4]. As shown in Fig. 1(a) this decay proceeds via an internal spectator diagram, and is "color-suppressed" since the color of the quarks produced by the weak current must correspond to the color of the c quark and the spectator quark. Recent measurements [5] of the branching fractions for the color-suppressed decays $\bar{B}^0 \to D^0X^0$, where $X^0 = \pi^0, \eta$ or ω, are all higher than theoretical

predictions [6] providing evidence for failure of the naïve factorization model and suggesting sizable final state interactions (FSI). In the heavy quark limit, the QCD factorization model works effectively for color-allowed decays, while color-suppressed decays require substantial correction [7]. Assuming SU(3) symmetry for the FSI rescattering phase, the observed discrepancy can be accommodated and branching fractions, such as $\mathcal{B}(\bar{B}^0 \to D^0\rho^0)$, can be predicted [8]. It is important to test whether $\bar{B}^0 \to D^0\rho^0$, once observed, supports the current pattern of QCD effects in color-suppressed B decays.

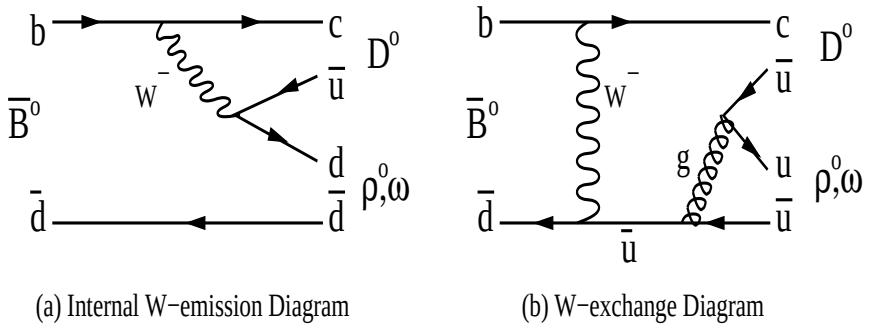

Fig. 1. Decay diagrams for $\bar{B}^0 \to D^0\rho^0, D^0\omega$.

The dominant diagrams for such neutral B meson decays preserve the spectator d-quark and therefore require that the final state neutral light meson be produced via its $d - \bar{d}$ component (Fig. 1(a)). These diagrams predict equal branching fractions for $D^0\rho^0$ and $D^0\omega$ and for $D^{*0}\rho^0$ and $D^{*0}\omega$. Other diagrams, such as W-exchange (Fig. 1(b)) or final state interactions can produce the $u - \bar{u}$ state and therefore give different branching fractions. This equality is therefore a very sensitive test for small amplitudes in which the spectator d-quark does not appear in the final state and the ρ or ω are produced via their $u - \bar{u}$ components [8,9].

In this paper, we will report on the study of $\bar{B}^0$ decays that have one D^0 or D^{*0} and two oppositely charged pions in the final state. Inclusion of charge conjugate modes is implied throughout this paper.

2 Data Sample and Selection Criteria

The data sample used in this paper was collected with the Belle detector at KEKB [10]. It is based on an integrated luminosity of 29.1 fb^{-1} at the $\Upsilon(4S)$ resonance, corresponding to 31.3 million $B\bar{B}$ events.

The Belle detector [11] is a large-solid-angle magnetic spectrometer that consists of a three-layer silicon vertex detector, a 50-layer central drift chamber (CDC), an array of aerogel threshold Čerenkov counters (ACC), a barrel-like

arrangement of time-of-flight scintillation counters (TOF), and an electromagnetic calorimeter comprised of CsI(Tl) crystals (ECL) located inside a super-conducting solenoid coil that provides a 1.5 T magnetic field. An iron flux-return located outside of the coil is instrumented to detect K_L^0 mesons and to identify muons (KLM).

Hadronic event selection is described elsewhere [12]. π^0 candidates are formed by combining two photons detected in the ECL, whose invariant mass is within a ± 16 MeV/c^2 mass window around the π^0 peak. The π^0 daughter photons are required to have energies greater than 20 MeV. We require the point of closest approach to the origin of each track to be within ± 5 mm from the beam axis and ± 3 cm along the beam axis from the interaction point to remove background. Tracks identified as electrons (from the responses of the CDC and ECL) or muons (from the response of the KLM) are removed. Kaon and pion candidates are distinguished by combining the dE/dx information from the CDC, time of flight information from the TOF and hit information from the ACC.

D^0 candidates are reconstructed in the decay modes $K^-\pi^+$, $K^-\pi^+\pi^0$, and $K^-\pi^+\pi^-\pi^+$. For $D^0 \to K^-\pi^+\pi^0$, the π^0 daughter photons are required to have energies greater than 50 MeV and we select regions of the Dalitz plot with large decay amplitudes to further suppress the combinatorial background [13]. The invariant masses of D^0 candidates are required to be within 2.5σ of the nominal mass. The selected π^0s and D^0s are then kinematically fit with their masses constrained to their nominal values [14]. D^{*0} candidates are formed by combining D^0 and π^0 candidates and selecting those with mass difference $\delta m = M_{D^{*0}} - M_{D^0}$ in the range $0.1400\ \mathrm{GeV}/c^2 < \delta m < 0.1445\ \mathrm{GeV}/c^2$.

3 B Meson Reconstruction

After selecting D^0 and D^{*0} candidates, we combine them with two oppositely charged pions to form B candidates. The two oppositely charged candidate pions from the B decay are required to come from a single vertex. To remove K_S^0 candidates from the sample, the distance of the $\pi^+\pi^-$ vertex from the beam interaction point in the $r-\phi$ plane is required to be less than 0.8 cm. Two kinematic variables are used to identify signal candidates, the beam constrained mass, $M_{bc} = \sqrt{(E_{beam}^{CM})^2 - (P_B^{CM})^2}$, and the energy difference $\Delta E = E_B^{CM} - E_{beam}^{CM}$ where E_B^{CM} and P_B^{CM} are the center of mass (CM) energy and momentum of the $\bar{B}^0$ candidate, and $E_{beam}^{CM} = \sqrt{s}/2 = 5.29$ GeV. We select events with $|\Delta E| < 0.2$ GeV and $5.272\ \mathrm{GeV}/c^2 < M_{bc} < 5.288\ \mathrm{GeV}/c^2$ ($5.271\ \mathrm{GeV}/c^2 < M_{bc} < 5.289\ \mathrm{GeV}/c^2$) for $D^0\pi^+\pi^-$ ($D^{*0}\pi^+\pi^-$) final states. Further, if there are multiple B candidates in an event, we choose

the candidate with the smallest χ^2 combination,

$$\chi^2 = \chi^2_{D^0} + \chi^2_{\pi^+\pi^-}(+\chi^2_{\delta m}) \quad (1)$$

where, $\chi^2_{D^0}$ and $\chi^2_{\pi^+\pi^-}$ are obtained from D^0 and $\pi^+\pi^-$ vertex fitting respectively. For decay modes containing D^{*0}, $\chi^2_{\delta m}$— defined as the square of the difference of δm from its nominal value, in units of its resolution, $(\Delta(\delta m)/\sigma(\delta m))^2$— is additionally included in the best candidate selection requirement.

4 Background Suppression

Since the continuum background (arising from $e^+e^- \to q\bar{q}(q = u, d, c, s)$ transitions) has a different event topology, shape variables are very effective at improving the signal to noise ratio. Events are required to satisfy $R_2 < 0.5$, where R_2 is the ratio of the second Fox-Wolfram moment to the zeroth moment determined using charged tracks and unmatched neutral showers [15]. The angle between the B candidate direction and the thrust axis [16] of the rest of the event (θ_T) is required to satisfy $|\cos(\theta_T)| < 0.7$.

For the $\bar{B}^0 \to D^{(*)0}\pi^+\pi^-$ branching fraction measurements, we make no assumptions about the intermediate mechanism, except that we reject the large contribution from the well-established decay $\bar{B}^0 \to D^{*+}\pi^-$ to the $D^0\pi^+\pi^-$ final state. These events are rejected by requiring $M^2_{D^0\pi^+} > 4.62\,\mathrm{GeV}^2/c^4$ (Fig. 2), which removes 1% of the phase space for $\bar{B}^0 \to D^0\pi^+\pi^-$. As the decay $\bar{B}^0 \to D^*_2(2460)^+\pi^-$ is not well established [14], no attempt is made to reject it and this mode is thus included in our branching fraction measurement.

Color-favored decays can also cause a background when a final state pion is replaced by a pion from the decay of the other B (for example $B^- \to D^{(*)0}\rho^-$ may be reconstructed as $\bar{B}^0 \to D^{(*)0}\pi^+\pi^-$). To reduce this background we veto events which can also be reconstructed in a color-favored mode. This requirement removes 1% of the signal candidates. Using a sample of 44 million generic $b \to c$ decays generated via Monte Carlo (MC) simulation, the small remaining background is studied and found not to peak in M_{bc} or ΔE.

5 Branching Fractions for $D^0\pi^+\pi^-$ and $D^{*0}\pi^+\pi^-$ final states

The distribution in ΔE for the surviving candidates for $\bar{B}^0 \to D^0\pi^+\pi^-$ is shown in Fig. 3(a). Since intermediate resonances dominate the decay rate we

obtain a non-uniform distribution of events on the Dalitz plot. In addition, the efficiency varies across the Dalitz plot due to momentum dependences of the reconstruction and particle identification efficiencies. We divide the Dalitz plot into six different regions expected to be dominated by different intermediate processes as shown in Fig. 2 and determine the efficiency [17] and signal yield (from ΔE fit) for each. Table 1 summarizes our results.

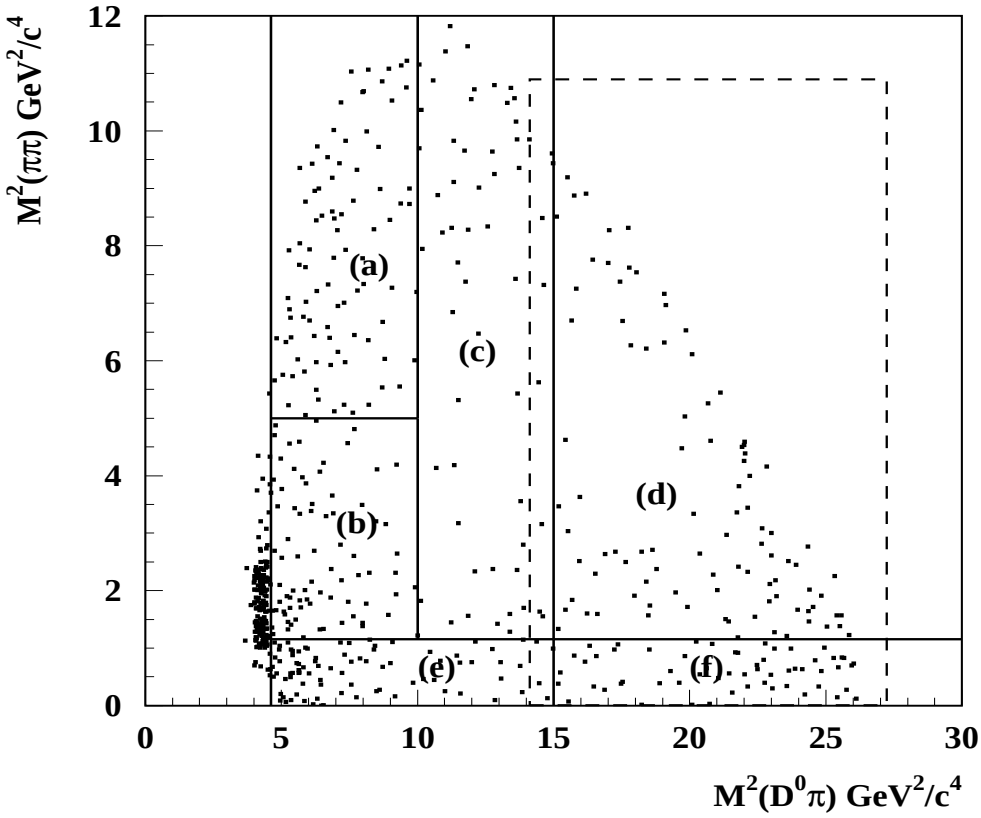

Fig. 2. Dalitz plot for $\bar{B}^0 \to D^0\pi^+\pi^-$ events with $|\Delta E| < 0.03$ GeV, showing the regions (a)-(f) used in the efficiency measurement. Events in the dashed box are used for the branching fraction measurement of $\bar{B}^0 \to D^0\rho^0$ as explained in the text.

For each Dalitz plot region we model the signal in ΔE with a Gaussian function where both the mean and width are fixed from MC studies. The background shape in this fit is modeled by two components: (1) a linear shape for continuum background obtained from the sideband data (5.20 GeV/c^2 < M_{bc} < 5.26 GeV/c^2); (2) a smooth histogram shape for $\bar{B}^0 \to D^{*0}\pi^+\pi^-$ feed-down obtained from MC. The normalizations of the signal and background

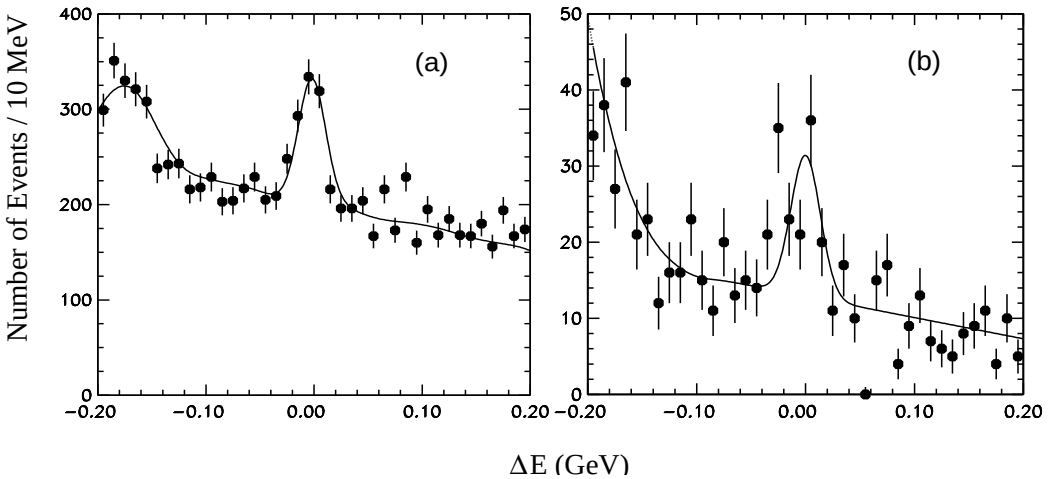

Fig. 3. (a) ΔE distribution for $\bar{B} \to D^0\pi^+\pi^-$ events satisfying $M^2_{D^0\pi^+} > 4.62$ GeV$^2/c^4$. (b) ΔE distribution for $\bar{B} \to D^{*0}\pi^+\pi^-$ candidates with no requirement on $M^2_{D^{*0}\pi^+}$.

Table 1
Summary of branching fraction results for $\bar{B}^0 \to D^0\pi^+\pi^-$ in different regions of the Dalitz plot. The last row gives the sums of the signal yields and branching fractions.

Region	Efficiency (%)	Signal Yield	Branching Fraction ($\times 10^{-4}$)
(a)	1.87 ± 0.09	98 ± 15	1.7 ± 0.3
(b)	1.66 ± 0.11	70 ± 18	1.3 ± 0.3
(c)	1.88 ± 0.08	17 ± 5	0.3 ± 0.1
(d)	1.94 ± 0.07	57 ± 15	0.9 ± 0.2
(e)	2.10 ± 0.17	76 ± 19	1.2 ± 0.3
(f)	1.85 ± 0.12	150 ± 16	2.6 ± 0.3
Total		469 ± 38	8.0 ± 0.6

components are free parameters in the fit. We obtain the branching fraction for $\bar{B}^0 \to D^0\pi^+\pi^-$ by taking the sum of the branching fractions in the six regions of the Dalitz plot and making a correction of 1% for the unobserved region where $M^2_{D^0\pi^+} < 4.62\,\mathrm{GeV}^2/c^4$. In all branching fraction calculations we assume equal production of $B^0\bar{B}^0$ and B^+B^- pairs from the $\Upsilon(4S)$.

To estimate the branching fraction for $\bar{B}^0 \to D^{*0}\pi^+\pi^-$ decays, we make no restriction on $M^2_{D^{*0}\pi^+}$. Due to limited statistics, we do not estimate the branching fraction region by region. Instead, we use the yield from the ΔE fit (Fig. 3(b)) and include a model dependent systematic error (19%) that arises from the difference between the detection efficiency when the signal MC events are $\bar{B}^0 \to D^{*0}\pi^+\pi^-$ and $\bar{B}^0 \to D^{*0}\rho^0$. The two detection efficiencies are 0.26%

and 0.32%, respectively where the $\bar{B}^0 \to D^{*0}\rho^0$ decay is generated with equal rates to each helicity state.

The background near the lower side of the ΔE distribution is modeled by $B^+ \to D^{*0}a_1^+$ feed-down measured using MC. The yield from the fit is 62 $\pm$ 12 events. We measure the branching fraction for $\bar{B}^0 \to D^{*0}\pi^+\pi^-$ using the phase space MC efficiency. The results are summarized in Table 2.

6 Search for Color-Suppressed $\bar{B}^0 \to D^{(*)0}\rho^0$ Decays

Multi-body decays of B mesons can occur through various strong resonances that can interfere with each other. We search for color-suppressed $\bar{B}^0 \to D^{(*)0}\rho^0$ decays in the $D^{(*)0}\pi^+\pi^-$ final state. We study the $\pi^+\pi^-$ invariant mass of the events in the signal region ($|\Delta E| < 0.030$ GeV for $D^0\pi^+\pi^-$ and $|\Delta E| < 0.035$ GeV for $D^{*0}\pi^+\pi^-$) and fit the ρ^0 yield with a relativistic Breit-Wigner function whose mean and width are fixed to the PDG values [14] to estimate the branching fraction.

To study the color-suppressed decay mode $\bar{B}^0 \to D^0\rho^0$, we require $M^2_{D^0\pi^+} > 14.0$ GeV$^2/c^4$ to remove backgrounds from $D^{*+}\pi^-, D_2^{*+}\pi^-$ decays and other D resonances. After this requirement, we clearly see an excess at the ρ^0 mass in the $\pi^+\pi^-$ invariant mass distribution (Fig. 4(a)). The excess around 1.45 GeV/c^2 can be modeled by either a $\rho(1450)$ or an $f_0(1370)$ resonance; we cannot discriminate between these states, or alternative models of the excess, based on the fit. Events near 0.5 GeV/c^2 may come from the σ [18] resonance. We extract the ρ^0 yield using a one dimensional likelihood fit. We use a model which includes one low mass and one high mass wide resonance. The masses and widths are fixed, and the amplitudes and phases are free parameters in the fit. The error from the fit therefore incorporates the error from the relative phases of the interfering terms: this tends to increase the error on the yield. The background under the signal events is described reasonably well by data from the ΔE sideband (0.06 GeV $< \Delta E <$ 0.20 GeV) shown as the hatched histogram in Fig. 4(a). We model this shape with a combination of phase space, a polynomial and a Breit-Wigner function, where the third term takes into account the possible contribution of true ρ^0 in the background. From the fit, we obtain 86 $\pm$ 30 signal events corresponding to a branching fraction of $\mathcal{B}(\bar{B}^0 \to D^0\rho^0) = (2.9 \pm 1.0 \pm 0.4)\times 10^{-4}$. The statistical significance of the signal, calculated as $\sqrt{-2\ln(L_0/L_{max})}$ where L_{max} is the likelihood with the nominal yield and L_0 is the likelihood with the signal constrained to be zero, is 6.1σ. We find a strong correlation between the amplitude of the ρ^0 component and its relative phase with respect to the higher mass resonance; if the amplitudes and phases of the high and low mass resonances are fixed at their obtained values, and the fit is repeated, a ρ^0 yield of 86$\pm$24 events is

obtained. We have repeated the fit with a number of different models including vector and scalar resonances at different masses and with different widths; the variation in the central value of the ρ^0 yield is negligible compared to the error from our default fit. As a further cross-check, we examine the the helicity angle (Θ_ρ), defined as the angle in the ρ^0 rest frame between the direction of the π^+ and the ρ^0 direction in the B rest frame, and find it to be consistent with the expected shape [19].

To extract the branching fraction of $\bar{B}^0 \to D^{*0}\rho^0$ we require $M^2_{D^{*0}\pi^+} > 6.3$ GeV$^2/c^4$, which removes backgrounds coming from $\bar{B}^0 \to D_2^*(2460)^+\pi^-$. We fit the $\pi^+\pi^-$ mass distribution using a relativistic Breit-Wigner function after fixing the background shape from the ΔE sideband (Fig. 4(b)). The ρ^0 event yield is 29 ± 8, however since the limited statistics prevent us from studying possible interferences with other resonances, we cannot interpret this as evidence for $D^{*0}\rho^0$ and we set an upper limit of the branching fraction. Assuming Gaussian statistics, we find $\mathcal{B}(\bar{B}^0 \to D^{*0}\rho^0) < 5.1 \times 10^{-4}$ at the 90% confidence level. We summarize our results in Table 2.

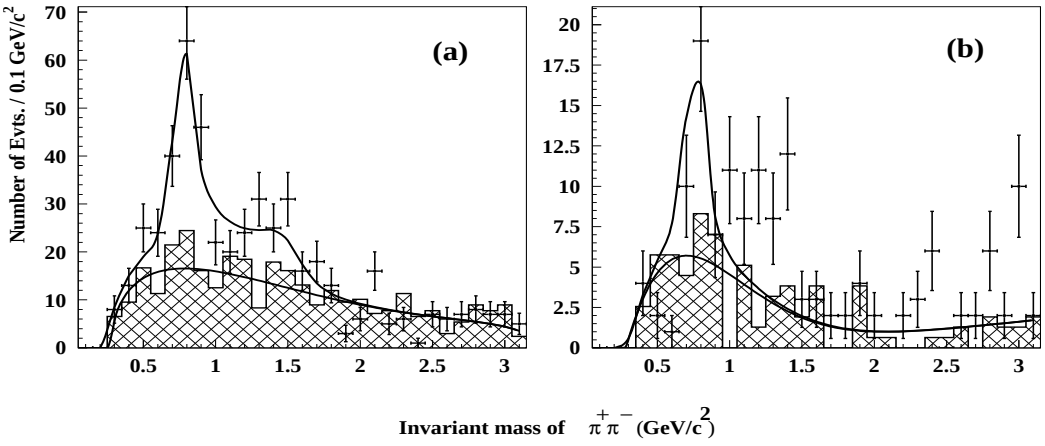

Fig. 4. $M_{\pi^+\pi^-}$ distribution from (a) $\bar{B}^0 \to D^0\pi^+\pi^-$ and (b) $\bar{B}^0 \to D^{*0}\pi^+\pi^-$ final states. The histogram represents the data from the ΔE sideband and the fit to the histogram is parameterized as described in the text.

Table 2
Summary of branching fraction results for $\bar{B}^0 \to D^{(*)0}\pi^+\pi^-$ and $\bar{B}^0 \to D^{(*)0}\rho^0$ [20].

Mode	Efficiency (%)	Branching Fraction ($\times 10^{-4}$)	Significance (σ)
$\bar{B}^0 \to D^0\pi^+\pi^-$	1.86	$8.0 \pm 0.6 \pm 1.5$	18.3
$\bar{B}^0 \to D^{*0}\pi^+\pi^-$	0.32	$6.2 \pm 1.2 \pm 1.8$	6.5
$\bar{B}^0 \to D^0\rho^0$	0.94	$2.9 \pm 1.0 \pm 0.4$	6.1
$\bar{B}^0 \to D^{*0}\rho^0$	0.24	< 5.1	-

The following sources of systematic error are considered in our measurements: (1) tracking efficiency (2.0% per track - measured by comparing the yield of the decay modes (i) $\eta \to \pi^0\pi^+\pi^-$ and (ii) $\eta \to \gamma\gamma$); (2) particle identification efficiency for π (4.3%); (3) D^0 reconstruction efficiency and decay branching fractions (12.7% - measured by comparing the observed yield of $B^- \to D^0\pi^-$ events with the expected yield using known branching fractions [14]); (4) slow π^0 efficiency (10.7% - measured from the ratio of branching fractions of $B^- \to D^0\pi^-$ and $B^- \to D^{*0}\pi^-$); (5) ΔE signal parameterization (typically 8%); (6) number of $B\bar{B}$ events (1.0%) and (7) MC statistics (3–5%). As described previously, an additional systematic error due to model dependence of the efficiency calculation is added for $\bar{B}^0 \to D^{(*)0}\pi^+\pi^-$. The total systematic error is obtained by combining the different contributions in quadrature.

7 Summary

In summary, we report the first observation of the color-suppressed $\bar{B}^0 \to D^0\rho^0$ decays and measure the branching fraction for $\bar{B}^0 \to D^{(*)0}\pi^+\pi^-$. Our measurement of $\mathcal{B}(\bar{B}^0 \to D^0\rho^0)$ is higher than the factorization prediction of 0.7×10^{-4} [6], thus continuing the trend mentioned in the introduction. When we compare the branching fraction of $\bar{B}^0 \to D^0\rho^0$ to our previous measurement of the branching fraction of $\bar{B}^0 \to D^0\omega$ [5], we obtain the ratio $\mathcal{B}(\bar{B}^0 \to D^0\rho^0)/\mathcal{B}(\bar{B}^0 \to D^0\omega) = 1.6 \pm 0.8$. The error includes both statistical and systematic errors where the correlation of the systematic errors has been taken into account. Future measurements with more statistics will allow precise tests of the mechanisms involved in color-suppressed B decays.

Acknowledgments

We wish to thank the KEKB accelerator group for the excellent operation of the KEKB accelerator. We acknowledge support from the Ministry of Education, Culture, Sports, Science, and Technology of Japan and the Japan Society for the Promotion of Science; the Australian Research Council and the Australian Department of Industry, Science and Resources; the National Science Foundation of China under contract No. 10175071; the Department of Science and Technology of India; the BK21 program of the Ministry of Education of Korea and the CHEP SRC program of the Korea Science and Engineering Foundation; the Polish State Committee for Scientific Research under contract No. 2P03B 17017; the Ministry of Science and Technology of the Russian Federation; the Ministry of Education, Science and Sport of the Republic of Slovenia; the National Science Council and the Ministry of

Education of Taiwan; and the U.S. Department of Energy.

References

[1] D. Fakirov and B. Stech, Nucl. Phys. B **133**, 315 (1978).

[2] C. Reader and N. Isgur, Phys. Rev. D **47**, 1007 (1993).

[3] M.S. Alam *et al.* (CLEO Collaboration), Phys. Rev. D **50**, 43 (1994).

[4] B. Nemati *et al.* (CLEO Collaboration), Phys. Rev. D **57**, 5363 (1998).

[5] K. Abe *et al.* (Belle Collaboration), Phys. Rev. Lett. **88**, 052002 (2002); T. E. Coan *et al.* (CLEO Collaboration), Phys. Rev. Lett. **88**, 062001 (2002).

[6] See, for example, M. Neubert *et al.*, hep-ph/9705292., in *Heavy Flavors*, edited by A. J. Buras and M. Lindner, 2nd ed. (World Scientific, Singapore).

[7] M. Neubert and A. A. Petrov, Phys. Lett. B **519**, 50 (2001).

[8] C.-K. Chua, W.-S. Hou and K.-C.Yang, Phys. Rev. D **65**, 096007 (2002).

[9] H. J. Lipkin, private communication.

[10] E. Kikutani ed., KEK Preprint 2001-157 (2001), to appear in Nucl. Instr. and Meth. A.

[11] A. Abashian *et al.* (Belle Collaboration), Nucl. Instr. and Meth. A **479**, 117 (2002).

[12] K. Abe *et al.* (Belle Collaboration), Phys. Rev. D **64**, 072001 (2001).

[13] S. Kopp *et al.* (CLEO Collaboration), Phys. Rev. D **63**, 092001 (1998).

[14] K. Hagiwara *et al.* (Particle Data Group), Phys. Rev. D **66**, 010001 (2002).

[15] The Fox-Wolfram moments were introduced in G. C. Fox and S. Wolfram, Phys. Rev. Lett. **41**, 1581 (1978).

[16] E. Farhi, Phys. Rev. Lett. **39**, 1587(1977).

[17] We generated 45,000 signal Monte Carlo events with a flat distribution in phase space to calculate efficiency in different regions of the Dalitz plot. We use the CLEO QQ generator; the detector response is simulated with GEANT, R. Brun *et al.*, GEANT 3.2.1, CERN Report DD/EE/84-1 (1984).

[18] E. M. Aitala *et al.* (E791 Collaboration), Phys. Rev. Lett. **86**, 770 (2001).

[19] Since B^0 and D^0 mesons are pseudoscalars, the ρ^0 mesons from $\bar{B}^0 \to D^0\rho^0$ decays will be longitudinally polarized giving a $\cos^2(\Theta_\rho)$ distribution.

[20] The significance for $\bar{B}^0 \to D^0\pi^+\pi^-$ is estimated by adding in quadrature the significances measured in each of the six Dalitz regions.